

PAPER • OPEN ACCESS

Hadron scattering, resonances, and QCD

To cite this article: R A Briceño 2016 *J. Phys.: Conf. Ser.* **770** 012024

View the [article online](#) for updates and enhancements.

Related content

- [Magnetic dipole and Gamow–Teller modes: quenching, fine structure and astrophysical implications](#)
A Richter
- [Multishell-model description of low-energy proton scattering](#)
J Stumm and A Hofmann
- [Pion scattering in \$^{208}\text{Pb}\$ and nuclear surface effects](#)
B Castel, P M Boucher and H Toki

Hadron scattering, resonances, and QCD

R A Briceño

Thomas Jefferson National Accelerator Facility,
12000 Jefferson Avenue, Newport News, VA 23606, USA

E-mail: rbriceno@jlab.org

Abstract. The non-perturbative nature of quantum chromodynamics (QCD) has historically left a gap in our understanding of the connection between the fundamental theory of the strong interactions and the rich structure of experimentally observed phenomena. For the simplest properties of stable hadrons, this is now circumvented with the use of lattice QCD (LQCD). In this talk I discuss a path towards a rigorous determination of few-hadron observables from LQCD. I illustrate the power of the methodology by presenting recently determined scattering amplitudes in the light-meson sector and their resonance content.

1. Introduction

The vast majority of hadronic states observed in nature are not stable under the strong interaction, but rather decay in the timescale of the interactions. As a result, these resonances do not live long enough to propagate and interact with particle detectors. Instead, their existence is manifested as dynamical enhancement of scattering amplitudes of their by-products - states composed of two or more hadrons. Therefore, to study the spectrum of the fundamental theory of the strong interactions, quantum chromodynamics (QCD), necessarily requires one to study few-body, strongly-interacting systems. In this talk I review some of recent progress towards achieving this goal directly from QCD and I focus my attention in the light sector of QCD [9, 8, 7, 14, 29, 28, 30, 13, 12], where calculations have reached a high level of maturity. In particular, I present the very first scattering amplitude in the isoscalar sector of QCD [9] and the first form factor of a resonance [8, 7]. These studies partly stem from formal theoretical developments which I briefly discuss [4, 17, 2, 5, 6].

Let me begin by focusing even further to two key examples. The first is perhaps the best understood hadronic resonance, namely the ρ . This resonance manifests itself as a “*bump*” in the isovector $\pi\pi$ scattering amplitude (or cross section), making it a perfect example of the common understanding of a resonance. This is nicely illustrated in Fig. 1, where one sees a clear enhancement in the $\pi\pi$ amplitude when the center of mass (cm) energy is in the proximity of 770 MeV. Unitarity dictates that the amplitude for the ℓ th partial wave can be written in terms of the scattering phase shift, δ_ℓ , $\mathcal{M}_\ell = \frac{8\pi E_{cm}}{p \cot \delta_\ell - ip}$, where E_{cm} and p are the c.m. energy and relative momentum. Using this, we find that the peak of this amplitude corresponds to approximately when the phase shift goes through 90° as seen in Fig. 1.

Although it is easy to understand resonances as bumps in amplitudes, this definition fails to describe some of the most interesting resonances in nature. To find a counterexample one can look in the isoscalar sector of QCD. This is perhaps one of the most interesting corners of QCD, as it includes tentative glueballs, molecules, tetraquarks, etc. Also, this sector hosts the lightest of all hadronic resonances, namely $\sigma/f_0(500)$. Although this plays an important role



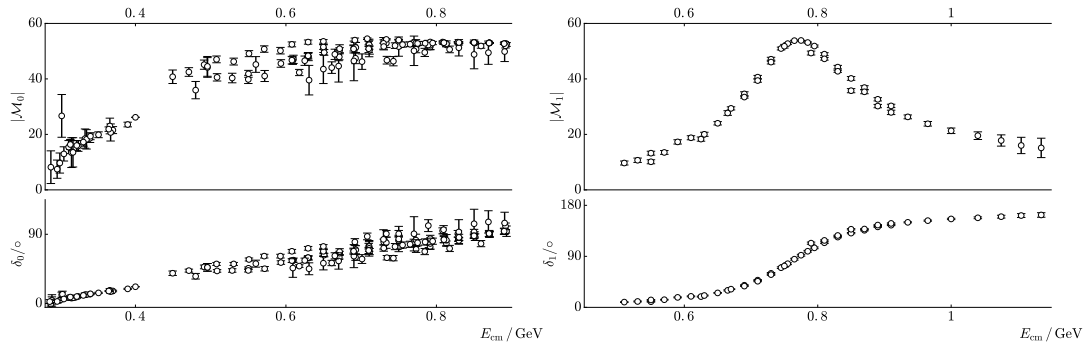


Figure 1. The top left and right panels respectively show the $\pi\pi$ isoscalar and isovector scattering amplitudes obtained from experiment [26, 20, 16, 15]. The bottom panels show the corresponding phase shifts.

in a wide range of phenomenology (see Ref. [25] for a recent review), it was not until recently that its existence was demonstrated with reliable certainty. As shown in Fig. 1, the reason the evidence for this state has been controversial is due to the absence of a bump-like signature in the low-energy region of the isoscalar $\pi\pi$ scattering amplitude. This is perhaps most striking when one realizes that its mass is $m_\sigma = 449^{(22)}_{(16)}$ MeV, which is smaller than its decay width $\Gamma_\sigma = 550(24)$ MeV [25].

Resonances can be rigorously defined as complex poles in scattering amplitudes. The imaginary and real components of these poles are directly related to their mass and width, $E_{pole} = \sqrt{s_{pole}} = m_R \pm i\Gamma_R/2$. It is easy to convince oneself that this definition is consistent with the picture of a resonance as a bump in a scattering amplitude when the width of the resonance is small compared to its mass. In the remainder of this talk, I review how resonant and non-resonant scattering amplitudes can be determined from lattice QCD. In Sec. 2, we will implement this methodology to determine the isovector and isoscalar $\pi\pi$ scattering amplitude. Having determined these amplitudes we will examine their pole structure and consequently their resonance content. In Sec. 3, I explain how these ideas are being extended to processes involving electroweak probes and present the first determination of a resonance form factor from lattice QCD [8, 7].

2. Scattering amplitudes from lattice QCD

In order to define lattice QCD, it is necessary to make four important compromises: nonzero lattice spacing, Wick rotation to a Euclidean spacetime, finite spacetime, and unphysical values for the quark masses. The first of these introduces a separation between all points in spacetime, and as a result spacetime resembles a crystal lattice. The second is done in order to use Monte Carlo sampling. The third is necessary to be able to store gauge fields, propagators, etc, which scale with the volume $(L^3 \times T)^2$ assuming a cubic volume, where L and T are the spatial and temporal extents. The last one has been a historical limitation that has been circumvented for the simplest of observables. In this talk I focus on few-body systems, where calculations are still in the exploratory stages and still being performed using unphysically heavy values for the quark masses.

For the physics we are after discretization effects are negligible and will be ignored. Naïvely one might consider the second and third compromises above as limitations, but these play a crucial role in the determination of few-body observables. First, the fact that the spacetime is finite leads to a discrete spectrum. Second, the fact that calculations are performed in a Euclidean spacetime allows us to identify correlation functions as sums of exponential whose arguments depend on the discrete spectrum. For example, the two-point correlation

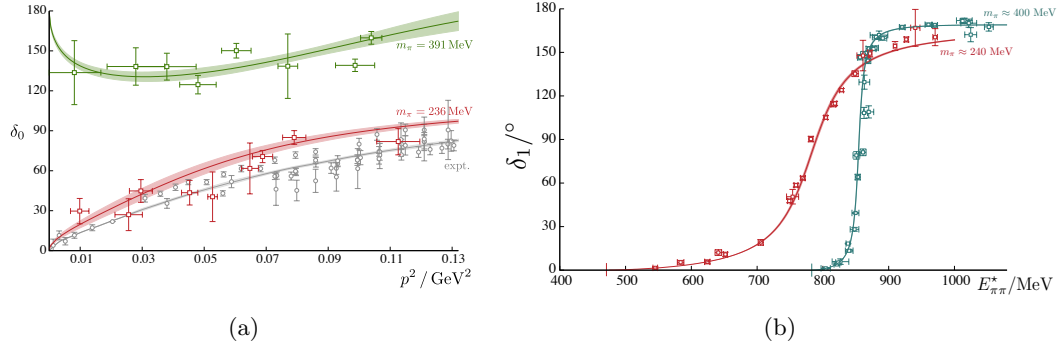


Figure 2. Shown are the lattice results for the elastic $\pi\pi$ scattering phase shifts in the (a) isoscalar [9] and (b) isovector channels [29, 12]. The isoscalar and isovector channels are plotted as a function of the c.m. relative momentum and energy respectively. These have been determined using two values of the quark masses, and the isoscalar is compared with the experimental values [26, 20, 16, 15].

function for a source $\mathcal{O}_a^\dagger(0)$ at time $t = 0$ and a sink operator $\mathcal{O}_b(t)$ can be written as, $C_{ab}^{2pt.}(t) \equiv \langle 0 | \mathcal{O}_b(t) \mathcal{O}_a^\dagger(0) | 0 \rangle = \sum_n Z_{b,n} Z_{a,n}^* e^{-E_n t}$, where E_n is the n th eigenvalue of the finite-volume Hamiltonian, $Z_{b,n}$ and $Z_{a,n}^*$ are the overlap factors with the sink and source operators respectively.

For a state whose energy lies well below multiparticle thresholds, the finite-volume energy can be identified as its infinite-volume counterpart up to corrections of the order of $\mathcal{O}(e^{-m_\pi L})$ [21]. For volumes satisfying $m_\pi L \gg 1$ one can safely neglect such corrections. For states above multiparticle thresholds there is no direct relation between finite-volume and infinite-volume states. This is easy to understand when one remembers that in the infinite-volume limit, states above thresholds are necessarily resonances and they correspond to complex poles on the second Riemann sheet. In a finite-volume, since there is not a continuum of states there is no branch cut. This means that there is a single Riemann sheet, and due to causality all states must lie on the real axis.

Instead one can non-perturbatively relate the finite-volume spectrum to the infinite-volume scattering amplitude. For two-particle systems such a relation was first found by Martin Lüscher [22, 23] and has been generalized to increasingly complex two-particle systems [22, 23, 4, 17, 2]. In general, one can find that an energy level in between the two- and three-particle thresholds satisfies, $\det[F^{-1}(P, L) + \mathcal{M}(E_L)] = 0$, where $F(E_L, L)$ is a known function of the spectrum and the volume [2] and \mathcal{M} is the scattering amplitude we are after. The determinant acts in the space of open channels and partial waves. For sufficiently low energies where a single partial wave dominates, it is straightforward to show that this equation simplifies down to where $\cot \phi(P, L)$ is related to $F(E_L, L)$.

Using this equation one can then directly map a finite-volume energy obtained from lattice QCD onto the infinite-volume scattering phase shift of the given channel evaluated at that same energy. This is what has been done in Refs. [9, 29, 12] for the isoscalar and isovector $\pi\pi$ channels using two different values of the light quark-masses corresponding to $m_\pi \approx 236, 391 \text{ MeV}$. The resulting phase shifts and fits are shown in Fig. 2. From the isovector phase shifts, it is evident that for these quark-masses the ρ resonance is fairly narrow and broadens as the quark-masses approach their physical value. This is as one would expect, given that as the quarks become increasingly light the phase space for the ρ to decay opens up. For the isoscalar phase shifts, the σ is bound for the heavy quark-masses, which is manifested by the phase shift starting at 180° . For the lighter ensemble, just like in experiment, it is less clear what the manifestation

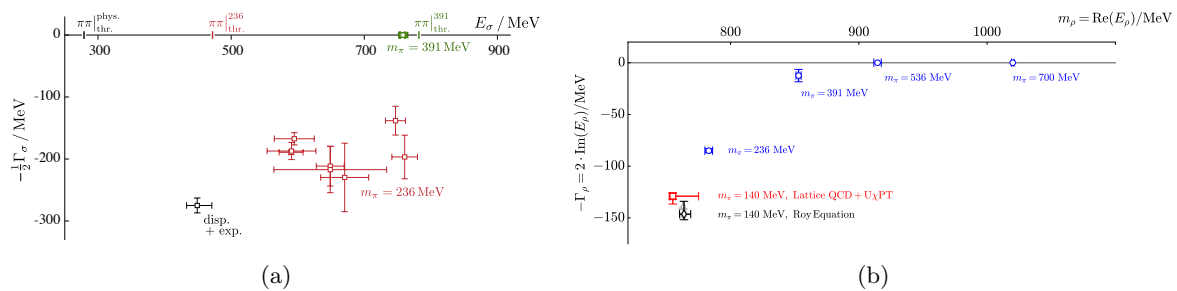


Figure 3. (a) Shown is the mass and width of the σ resonance for the two values of the quark masses studied via lattice QCD [9] and it is compared to the results from dispersive analysis of experimental data [25]. (b) Shown are the same quantities for the ρ [29, 12, 11], including a chiral extrapolation in red [1] and the result from dispersive analysis in black.

of the σ is, except one can conclude it is not a narrow resonance.

In Ref. [1] a chiral extrapolation of the isovector scattering amplitude was performed. The resulting amplitude was in good agreement with experimental values up to c.m. energies of 1.2 GeV, well above several inelastic thresholds. This confirms that inelastic effects can be safely ignored for this channel for a large kinematic region. Although a chiral extrapolation of the isoscalar amplitude is presently missing, in Fig. 2(a) one sees a natural trend for the phase shift from heavy quark masses down to the experimental point [26, 20, 16, 15].

To rigorously study the resonant content of these amplitudes, one must investigate their pole structure in the complex plane. Since lattice QCD energies are real, the scattering amplitude is only constrained on the real axis. To analytically continue onto the complex plane, one must rely on parametrizations of the scattering amplitude. Using a wide range of these, described in Ref. [30], one sees in Fig. 3 the resulting pole locations described in terms of the masses and widths of the σ and ρ resonances. First, let's focus on the ρ poles, which also include values of quark-masses where it is bound [11]. The red point depicts the pole position obtained after performing a chiral extrapolation of the $m_\pi = 236$ MeV ensembles [1], and it is in good agreement with solutions to the Roy equation constrained from experimental data. This figure reemphasizes the transition of the ρ from a stable particle to an increasingly broad resonance.

By performing calculations at sufficiently heavy values of the quark-masses, the σ is found to be bound [9]. This is perhaps the first clear evidence of the existence of the σ from QCD. As m_π approaches its physical value, the phase space for the σ to decay quickly opens and it becomes a broad resonance resembling the experimental situation. Given that this corresponds to a pole far from the real axis where the scattering amplitude has been constrained, it should not be a surprise that there might be a large systematic error associated with the parametrization chosen to perform such an extrapolation. This is represented by the scattered red points in Fig. 3(a). This systematic error can be dramatically reduced by using dispersive techniques, as has been done to analyze experimental data [25].

I end this section by making a couple of remarks. First, it is important to emphasize that determining the isoscalar finite-volume spectra, and even more the corresponding scattering amplitudes, directly from QCD is a technological achievement. Having obtained these amplitudes, the determination of resonances closely mirrors experimental analysis. As we approach the physical point, the analysis becomes increasingly complex, just as in experiment. Lattice QCD does possess one advantage over experiment. This is the fact that one can ‘*dial*’ the parameters of the standard model, in particular the quark masses. This allows one to see direct evidence of states whose experimental signature might be small, the σ being a perfect example. Second, although I have only discussed kinematic regions where a single channel is open, these

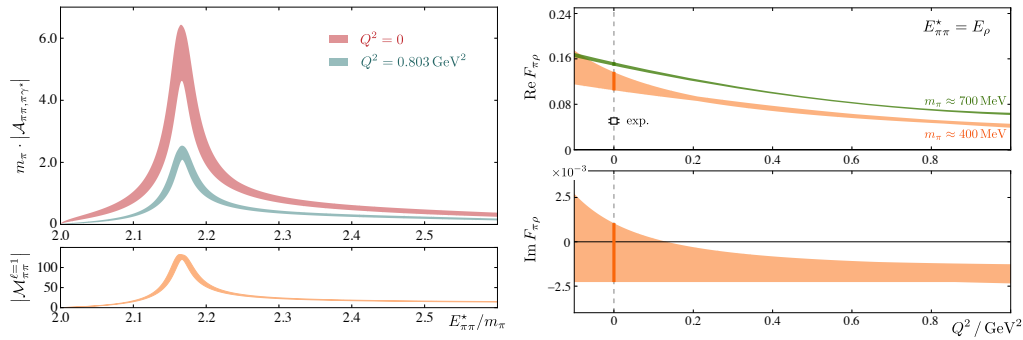


Figure 4. (a) Shown is the absolute values of the $\pi^+\gamma^* \rightarrow \pi^+\pi^0$ amplitude, $A_{\pi\pi,\pi\gamma^*}$ as a function of the $\pi\pi$ c.m. energy for two different Q^2 [8, 7], and it is compared to the elastic $\pi\pi$ amplitude below [12]. (b) Shown are the real and imaginary components of the $\pi \rightarrow \rho$ form factor for $m_\pi \approx 400 \text{ MeV}$ [8, 7], and it is compared to its value at $m_\pi \approx 700 \text{ MeV}$ [28].

ideas are also applicable for energies more channels are open. In fact the very first calculations involving more than open channel have been carried recently [14, 29, 30, 13]. Lastly, these ideas are also applicable in the heavy sector, and the very first coupled-channels calculations involving a heavy quark has been performed [24].

3. Electroweak processes from lattice QCD

In the previous section, I discussed how scattering amplitudes can be determined from lattice QCD. From these one can determine masses, decay widths, and strong couplings of hadronic resonances. As discussed above, these amplitudes are only accessible from lattice QCD, in part, due to the finite-volume formalism discussed above. It has recently been demonstrated how these ideas can be extended to the study of electroweak processes [5, 6, 27]. In particular, Refs. [5, 6] demonstrated how resonant $0 \rightarrow 2$ and $1 \rightarrow 2$ amplitudes in the presence of an external electroweak current can be extracted from lattice QCD, and Ref. [27] demonstrated how $2 \rightarrow 2$ amplitudes in the presence of an external current can be studied. From the residue of these amplitudes evaluated at the resonance poles, one can then rigorously define and determine the form factors of hadronic resonances.

In order to test these ideas, in Ref. [8, 7] an exploratory calculation of the $\pi^+\gamma^* \rightarrow \pi^+\pi^0$ amplitude was performed using a value of $m_\pi \approx 396 \text{ MeV}$. This amplitude was determined for a range of values of the c.m. energy and virtuality of the photon. Figure 4 shows a result of the global fit to the amplitude as a function of energy and two specific values of the virtuality. One sees a clear enhancement due to the presence of the ρ resonance. By analytically continuing the amplitude onto the resonance pole, the real and imaginary components of the $\pi \rightarrow \rho$ form factor were obtained and are shown in the same figure. These are compared with a previous calculation performed using $m_\pi \approx 700 \text{ MeV}$, where the ρ is stable [28]. Beyond testing these formal ideas, this calculation constitutes the first determination of a resonance form factor from lattice QCD.

4. Final Remarks and Outlook

In this talk I have discussed some recent developments in the study of scattering and resonances from lattice QCD. Two-body elastic and inelastic scattering amplitudes are now being determined, albeit at unphysically heavy quark masses. From these one can unambiguously determine masses and widths of hadronic resonances, and I have presented the very first rigorous study of the lightest of all hadronic resonances, the σ . Also, I discussed how these ideas are being extended to the study of few-body amplitudes involving electroweak currents, and I focused its application on the resonant $\pi^+\gamma^* \rightarrow \pi^+\pi^0$ amplitude.

Beyond the application of these ideas to other sectors of QCD, for example the charm sector [24], these ideas will allow for the determination of phenomenologically interesting observables that are not directly accessible from experiment. One such example is in the study of elastic form factors of resonances [27]. The implementation of this formalism will allow us to peer inside resonances and be able to describe their inner structure, very much as is already being done for the study of stable states. Presently these ideas are being extended to allow the study of systems where three particles can go on-shell [19, 18, 10, 3]. This will allow for a QCD determination of, for example, the three-neutron force as well as resonances that couple strongly to three-body final states, such as the Roper.

Acknowledgments

I would like to thank my colleagues within the Hadron Spectrum Collaboration, in particular Jozef Dudek, Robert Edwards, Christian Shultz, Christopher Thomas and David Wilson, as well as my other collaborators, Daniel Bolton and Maxwell Hansen, whose hard work made the results being presented possible. The work presented was partly supported by the U.S. Department of Energy contract DE-AC05-06OR23177, under which Jefferson Science Associates, LLC, manages and operates Jefferson Lab.

References

- [1] Daniel R. Bolton, Raul A. Briceño, and David J. Wilson. *Phys. Lett.*, B757:50–56, 2016.
- [2] Raul A. Briceño. *Phys.Rev.*, D89(7):074507, 2014.
- [3] Raul A. Briceño and Zohreh Davoudi. *Phys.Rev.*, D87:094507, 2012.
- [4] Raul A. Briceño and Zohreh Davoudi. *Phys. Rev. D*, 88, 094507:094507, 2013.
- [5] Raúl A. Briceño and Maxwell T. Hansen. *Phys. Rev.*, D92(7):074509, 2015.
- [6] Raul A. Briceño, Maxwell T. Hansen, and Andr Walker-Loud. *Phys.Rev.*, D91(3):034501, 2015.
- [7] Ral A. Briceño, Jozef J. Dudek, Robert G. Edwards, Christian J. Shultz, Christopher E. Thomas, and David J. Wilson. *Phys. Rev.*, D93(11):114508, 2016.
- [8] Raul A. Briceño, Jozef J. Dudek, Robert G. Edwards, Christian J. Shultz, Christopher E. Thomas, and David J. Wilson. *Phys. Rev. Lett.*, 115:242001, 2015.
- [9] Raul A. Briceño, Jozef J. Dudek, Robert G. Edwards, and David J. Wilson. 2016.
- [10] Raul A. Briceño, Maxwell T. Hansen, and Stephen R. Sharpe. 2016.
- [11] Jozef J. Dudek, Robert G. Edwards, Peng Guo, and Christopher E. Thomas. *Phys. Rev.*, D88(9):094505, 2013.
- [12] Jozef J. Dudek, Robert G. Edwards, and Christopher E. Thomas. *Phys.Rev.*, D87:034505, 2013.
- [13] Jozef J. Dudek, Robert G. Edwards, Christopher E. Thomas, and David J. Wilson. *Phys. Rev. Lett.*, 113(18):182001, 2014.
- [14] Jozef J. Dudek, Robert G. Edwards, and David J. Wilson. *Phys. Rev.*, D93(9):094506, 2016.
- [15] P. Estabrooks and Alan D. Martin. *Nucl. Phys.*, B79:301, 1974.
- [16] G. Grayer et al. *Nucl. Phys.*, B75:189–245, 1974.
- [17] Maxwell T. Hansen and Stephen R. Sharpe. *Phys.Rev.*, D86:016007, 2012.
- [18] Maxwell T. Hansen and Stephen R. Sharpe. *Phys.Rev.*, D90(11):116003, 2014.
- [19] Maxwell T. Hansen and Stephen R. Sharpe. *Phys. Rev.*, D92(11):114509, 2015.
- [20] B. Hyams et al. *Nucl. Phys.*, B64:134–162, 1973.
- [21] M. Luscher. *Commun.Math.Phys.*, 104:177, 1986.
- [22] M. Luscher. *Commun.Math.Phys.*, 105:153–188, 1986.
- [23] Martin Luscher. *Nucl.Phys.*, B354:531–578, 1991.
- [24] Graham Moir, Michael Peardon, Sinad M. Ryan, Christopher E. Thomas, and David J. Wilson. 2016.
- [25] J. R. Pelaez. 2015.
- [26] S.D. Protopopescu, M. Alston-Garnjost, A. Barbaro-Galtieri, Stanley M. Flatte, J.H. Friedman, et al. *Phys.Rev.*, D7:1279, 1973.
- [27] Raúl A. Raúl and Maxwell T. Hansen. *Phys. Rev.*, D94(1):013008, 2016.
- [28] Christian J. Shultz, Jozef J. Dudek, and Robert G. Edwards. *Phys. Rev.*, D91(11):114501, 2015.
- [29] David J. Wilson, Raul A. Briceño, Jozef J. Dudek, Robert G. Edwards, and Christopher E. Thomas. *Phys. Rev.*, D92(9):094502, 2015.
- [30] David J. Wilson, Jozef J. Dudek, Robert G. Edwards, and Christopher E. Thomas. *Phys. Rev.*, D91(5):054008, 2015.